Thermodynamic Modeling of the Adsorption of Radionuclides on Selected Minerals. II: Anions

ARTICLE *in* INDUSTRIAL & ENGINEERING CHEMISTRY RESEARCH · AUGUST 2001

Impact Factor: 2.59 · DOI: 10.1021/ie000992h

Thermodynamic Modeling of the Adsorption of Radionuclides on Selected Minerals. II: Anions

Peiming Wang* and Andrzej Anderko

OLI Systems, Inc., 108 American Road, Morris Plains, New Jersey 07950

David R. Turner

Center for Nuclear Waste Regulatory Analyses, Southwest Research Institute, 6220 Culebra Road, San Antonio, Texas 78238-5166

A surface complexation model based on the diffuse-layer theory has been applied to study the adsorption of radionuclide anions (I^-, IO_3^-, SeO_3^{2-}, SeO_4^{2-}, and TcO_4^-) on various minerals. The model is coupled with an aqueous activity coefficient model based on the B-dot equation and takes into account the effect of aqueous speciation on adsorption. Binding constants for the selected radionuclide anions on minerals have been determined. In all examined cases, the model is shown to accurately represent the adsorption data. The selected radionuclide anions have been identified as potentially significant contributors for dosing in high-level nuclear waste because of their high solubilities and reduced interactions with aquifer minerals; the methodology presented in this work can be generalized to the study of ion adsorption effects at water−mineral interfaces in natural systems that implicitly regulate the fate of environmental contaminants.

1. Introduction

Sorption of radionuclides is an important issue in various fields including water and wastewater treatment, environmental science, materials science, analytical chemistry, and geochemistry. In the geologic disposal of high-level nuclear waste (HLW), migration of radionuclides dissolved in groundwater through the geosphere is one of the principal measures of repository performance. Radionuclide sorption onto minerals is a process that can contribute to the delay of radionuclide arrival or reduce their concentrations in groundwater at receptor locations that is of particular interest in HLW management. In the United States HLW program, the U.S. Department of Energy (DOE) is currently characterizing and evaluating a proposed repository site at Yucca Mountain, Nevada. The current U.S. Nuclear Regulatory Commission (NRC) regulations governing the licensing of any proposed repository at Yucca Mountain include a requirement that DOE demonstrate long-term repository performance using total system performance assessments. These performance assessments include simulations of potential radionuclide transport through the vadose zone and the local groundwater system[1,2] at Yucca Mountain. As part of the NRC review and evaluation of the adequacy of any DOE license application, NRC staff will need to understand the role of processes that might contribute to radionuclide retardation and how these processes are simulated in the DOE performance assessment. Radionuclide sorption is strongly dependent on the physicochemical conditions along the groundwater flow path. Understanding radionuclide sorption behavior on various minerals is necessary for predicting the behavior of radionuclides in natural environments.

A number of studies have provided data on radionuclide sorption over a wide range of chemical conditions.[3−16] Model approaches for the interpretation of these data have also been reported.[17−25] These studies provide a strong basis for developing uniform, detailed geochemical sorption models to support HLW assessment.

Recently, we have interpreted sorption data for radionuclides, selected for their significance in HLW disposal, using a thermodynamically consistent model that couples the diffuse-layer theory for surface complexation with an aqueous activity coefficient model based on the "B-dot" method of Helgeson[26] for aqueous speciation calculations.[27] A model was developed based on the work of Turner and Sassman[23] on defining the acid−base behavior of minerals. In this paper, we report the application of this model to study the sorption of radionuclides typically present in groundwater as anions. Negatively charged anions generally interact weakly with silicate and oxide minerals; this limited sorption makes many anionic contaminants more mobile and of particular concern in transport analyses.

Iodine, technetium, and selenium are potentially significant contributors to dosing in HLW. In oxidizing natural waters, these radionuclides exist as anionic species such as I^-, IO_3^-, SeO_3^{2-}, SeO_4^{2-}, and TcO_4^- that can form highly soluble salts and are poorly retarded by geological barriers. Recent assessment calculations of the proposed HLW repository at Yucca Mountain, Nevada, identify ^{79}Se, ^{99}Tc, and ^{129}I as critical radionuclides for repository performance.[28−30] For a regulatory time frame of 10^4 years, ^{99}Tc and ^{129}I are the major contributors to dosing.[28−30] The sorption behavior of these radionuclides is dependent on geochemical conditions such as pH. In addition, the redox conditions of the groundwater system are important; for example, Tc exists in a heptavalent (7+) state under nonreducing conditions as the pertechnetate (TcO_4^-) anion. Under

* To whom correspondence should be addressed. E-mail: Pwang@olisystems.com. Tel.: 973-539-4996. Fax: 973-539-5922.

10.1021/ie000992h CCC: $20.00
Published on Web 08/30/2001

reducing conditions, however, Tc is present in a tetravalent (4+) state, with a lower solubility and stronger sorption characteristics.[31,32] Similar redox dependency has been discussed for selenium sorption.[33]

Because of its significance as a toxic metal in agricultural and industrial processes, a relatively large amount of sorption data has been reported for selenium, whereas only limited data are available for iodine and technetium. The available literature data constitute a sound database for the application of detailed models to evaluate the sorption behavior of anionic species in radioactive wastewaters.

The objectives of this work are (1) to evaluate published data on the sorption behavior of anionic radionuclide species using a thermodynamic model based on the diffuse-layer theory and aqueous speciation computations; (2) to develop consistent model parameters that can be used to support radionuclide transport calculations and, in hydrogeochemical surface complexation calculations, to account for radionuclide sorption; and (3) to predict the effect of system chemistry on the sorption of anionic species. It is also of interest to compare the results obtained from this study with those obtained for radionuclide cation adsorption,[27] to draw general conclusions with regard to the differences and similarities in sorption behavior for different radionuclides.

2. Modeling of Radionuclide Anion Adsorption Using the Surface Complexation Model

General Description. For consistency of approach, the surface complexation model (SCM)[34,35] used in the study of radionuclide cation sorption[27] was applied here. The model couples a diffuse-layer theory for surface complexation with an aqueous activity coefficient model based on the B-dot method of Helgeson[26] for aqueous speciation calculations.[27] The use of the B-dot activity coefficient model offers the possibility of extending the applicability of the model to a wider range of systems with higher ionic concentrations and with significant temperature variations.[27] Optimum values for surface complex binding constants were determined from published experimental sorption data using the general nonlinear least-squares optimization program FITEQL, version 2.0,[36,37] revised to incorporate the B-dot equation for aqueous activity coefficients.[27] As appropriate, the acid−base behavior of minerals has been based on the work of Turner and Sassman.[23] Acidity constants for additional minerals not considered by Turner and Sassman[23] (e.g., cinnabar and chalcocite) were determined using the diffuse-layer model (DLM) with published potentiometric titration data.[5] A single site type and a single site density value (2.31×10^{18} site/m^2) were assumed in the model because of the lack of data on site heterogeneities for many of the minerals considered in this study.[27] The aqueous speciation equilibrium constants used in the chemical model were taken from the Data0.com.V8.R6 file of the EQ3/6 thermodynamic database[38,39] and are listed in Table 1. Details of the model were presented in Part I of this study in the preceding paper.[27]

Sorption modeling involves adjusting the binding constants for one or more postulated surface reactions to minimize the differences between experimental and calculated values of the sorbed amount of radionuclide at each pH under defined physical and chemical conditions such as ionic strength (I), total radionuclide concentration (C_{RN}), solid mass-to-solution volume ratio (m/V), and mineral specific surface area (A_{sp}). Although spectroscopic techniques such as extended X-ray absorption fine structure (EXAFS) potentially can be used to identify surface species, data are not available for I, Tc, and Se, so the selection of surface species is based primarily on an analysis of aqueous speciation and the results of the sorption data regression.

Table 1. Aqueous Reactions Associated with Iodate, Se(VI), and Se(IV) and Their Equilibrium Constants at 25 °C[a]

aqueous reactions	log K
$IO_3^- + H^+ = HIO_3^0$	0.49
$SeO_4^{2-} + H^+ = HSeO_4^-$	1.91
$SeO_3^{2-} + H^+ = HSeO_3^-$	7.29
$SeO_3^{2-} + 2H^+ = H_2SeO_3^0$	9.86

[a] Equilibrium constants were based on thermodynamic data from Data0.com.V8.R6 file of the EQ3/6 database.[38,39]

Evaluation of Radionuclide Sorption Data for Modeling. Using a variety of published sources, sorption data for I^-, IO_3^-, SeO_3^{2-}, SeO_4^{2-}, and TcO_4^- that cover a wide range of chemical conditions were selected for the modeling. These data were measured under specified conditions of pH, I, C_{RN}, m/V, and A_{sp}. Although it is difficult to assess the uncertainties of the reported sorption data, the guidelines described by Dzombak and Morel[34] for error estimates are used in the present study in the parameter regression.

Frequently, only one data set is available at a single set of experimental conditions for a given radioelement−mineral system, but there are cases where two or more sources are available for a specific system. For example, sorption data for selenite on goethite have been reported by Balistrieri and Chao,[3] Zhang and Sparks,[16] and Parida et al.[12] In these cases, each data set has been treated separately to determine the optimal binding constants. Generally, binding constants determined from multiple data sets are in reasonably good agreement in this study. However, of the three data sources for the sorption of selenite on goethite, the data of Parida et al.[12] show considerably lower sorption under conditions comparable to those of Balistrieri and Chao[3] and of Zhang and Sparks.[16] The Parida et al.[12] data were not considered in the determination of the binding constants for the selenium−goethite system.

Several sets of data for iodine sorption on minerals such as hematite,[6] cinnabar,[5,9] and chalcocite[5] are among those selected for this study. Couture and Seitz[6] also measured sorption for iodine on kaolinite, but the sorption was too low (e.g., <5% for the sorption of I^-), and the measurements contained too few points to constrain modeling parameters. Moreover, the observed sorption of iodine on silicate minerals has been suggested[6] to actually be due to sorption by iron oxide or other impurities. For this reason, these sorption data for iodine on kaolinite were not analyzed in this study. Sorption data were also reported for I^- on TiO_2 by Hakem et al.,[40] but the initial iodide concentration was not reported, making it impossible to use these data for developing a geochemical sorption model.

Sorption data for technetium are relatively scarse compared with those for the other radionuclides. Two data sets found for sorption of TcO_4^-[10,14] contain only a few data points each. Palmer and Meyer[11] measured pertechnetate sorption on a number of synthetic inorganic materials, including Al_2O_3, as well as on some naturally occurring minerals under various ionic strength

conditions. The sorption data were presented in terms of a distribution coefficient (K_d) vs pH. However, the original paper did not indicate the solid concentration (m/V) used in their experiments, which makes it impossible to convert K_d values to amounts of sorbed pertechnetate, which could then be used in the modeling. Therefore, the data of Palmer and Meyer[11] were not analyzed in this study.

Determination of Acidity Constants for Metal Sulfide Minerals. Metal sulfides have been recognized as important adsorbents in nature. Although iron sulfides are the most abundant metal sulfides in the earth's crust, their relatively high solubility compared to that of other metal sulfides and the formation of a series of metastable iron sulfide species,[41] have made the characterization and identification of the chemical species at their surfaces difficult. The development of surface charge at metal sulfide surfaces can be ascribed to multiple functional groups, such as the thiol group (≡SH) and the metal hydroxide group (≡Me−OH). The extreme insolubilities of cinnabar (HgS) and chalcocite (Cu_2S) make them good model surfaces for iron sulfides. The study of adsorption of radionuclides on these metal sulfides might provide valuable information for the characterization and identification of surface species that can form on iron sulfides.

SCM approaches have generally been used in the literature to model adsorption on hydrous oxide minerals.[34,35] To model the sorption of radionuclides on cinnabar and chalcocite, surface acidity constants for these two sulfides are needed. Using the potentiometric titration data of Balsley et al.,[5] DLM surface acidity constants for these two sulfides were determined using FITEQL (Figure 1). Cinnabar and chalcocite exhibit negative surface charge in the pH ranges of the potentiometric measurements (pH < 9).[5] Thus, only the deprotonation constants, K_{-}, were obtained. The values of these constants, together with their standard deviations, are given in Table 2. It should be noted that, in addition to thiol groups, hydroxyl groups can also exist at the hydroxylated surface sites and contribute to the surface charge. However, hydroxylated Cu(I) and Hg(II) only deprotonate in solution at very alkaline pH's.[42] The deprotonation of thiol groups might outweigh that of the hydroxylated sites under common groundwater pH conditions. The deprotonation constants obtained from our DLM approach perhaps reflect primarily the deprotonation of thiol groups on the metal sulfide surfaces. Deprotonation constants for cinnabar and chalcocite, together with aqueous reaction equilibrium constants, were used to determine binding constants for iodide on these two metal sulfides.

3. Results and Discussion

Representation of Experimental Data. The binding constants determined in this study for I, Se, and Tc are given in Tables 2−4. Also listed in these tables are the surface complexation reactions corresponding to the equilibrium binding constants and the intrinsic surface acidity constants used in the model. Standard deviations (σ) calculated by FITEQL for binding constants are also given.

In the case of multiple data sets, binding constants were first determined for each individual data set. The best estimates were then determined by a weighted average of the optimum log K value determined from each individual data set, as discussed by Dzombak and Morel.[34] The standard deviation of the average log K value was assigned to be equal to the largest σ from the individual data regressions. Although binding constants determined from multiple data sets are in reasonably good agreement with each other in most cases in this study, there are cases where inconsistency exists among data sets from different authors. For example, binding constants of selenite on goethite determined from the data of Balistrieri and Chao[3] [log $K(\equiv XOH_2-HSeO_3^0)$ = 18.83 (σ = 0.298) and log $K(\equiv XOH-HSeO_3^-)$ = 12.99 (σ = 0.068)] provide an excellent representation of experimental results at various selenite and solid concentrations. The same binding constants predict sorption that is about 10−15% lower than that indicated by the experimental data of Zhang and Sparks.[16] When determined using the Zhang and Sparks data,[16] these binding constants are significantly higher [log $K(\equiv XOH_2-HSeO_3^0)$ = 19.99 (σ = 0.392) and log $K(\equiv XOH-HSeO_3^-)$ = 14.35 (σ = 0.152)]. The difference in log K values determined from the two data sets might arise from sources of error in the two measurements due to the different experimental techniques. Binding constants determined from the Balistrieri and Chao[3] data are given in Table 3.

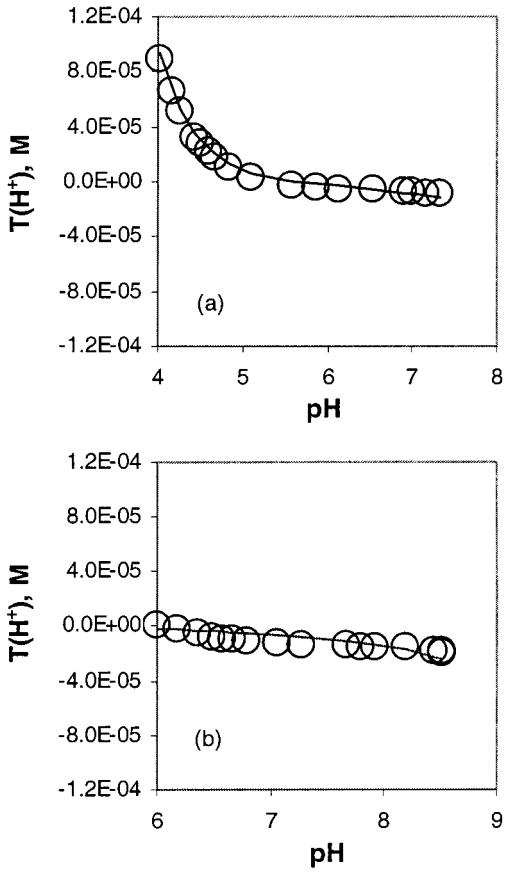

Figure 1. Potentiometric titration of (a) cinnabar and (b) chalcocite. The lines are calculated using parameters listed in Table 2, and experimental data are from Balsley et al. (1996)[5] (m/V = 50 g/L, A_{sp} = 1.99 m^2/g for cinnabar and A_{sp} = 1.11 m^2/g for chalcocite, I = 0.001 M NaCl).

Figures 2−14 compare the experimental and calculated sorption results for I^-, IO_3^-, SeO_3^{2-}, SeO_4^{2-}, and TcO_4^-. All of the lines in these figures were calculated using the binding constants obtained from the present study as listed in Tables 2−4. In general, The agreement between the experimental and calculated sorption results is good.

Table 2. Summary of Parameters Used for the Determination of Binding Constants for the Sorption of I^- and IO_3^- on Various Minerals[a]

radionuclide/solid	A_{sp} (m^2/g)	m/V (g/L)	C_{NR} (M)	I (M)	log K_+	log K_-	log K_1[b]	log K_2[b]	ref
IO_3^-/hematite (α-Fe_2O_3)	10	58.31	1.2×10^{-3}	0.112[c]	7.35[d]	−9.17[d]	2.00 (0.04)	8.43 (0.09)	6
I^-/cinnabar (HgS)	1.99	1.0	1.0×10^{-5}	0.01 (NaCl)	nc[e]	−7.27 (0.06)[f]	6.86 (0.06)	9.05 (0.11)	5
I^-/chalcocite (Cu_2S)	1.11	1.0	1.0×10^{-5}	0.01 (NaCl)	nc[e]	−6.95 (0.03)[f]	7.58 (0.05)	11.73 (0.14)	5

[a] A site density of 2.31 sites/nm^2 (from ref 34) was assigned to all minerals. [b] Binding constants K_1 and K_2 correspond to the following surface reactions: K_1, $\equiv XPH^0 + A^{-z} = \equiv XPH{-}A^{-z}$; K_2, $\equiv XPH^0 + A^{-z} + H^+ = \equiv XPH_2{-}A^{-z+1}$, where $A^{-z} = I^-$ or IO_3^-, P = O for hematite, and P = S for cinnabar and chalcocite. Values in parentheses are standard deviations of the binding constants. [c] 0.1 M $NaClO_4$ + 0.011 M $NaHCO_3$ + 0.0012 M KIO_3. [d] Acidity constants from Turner and Sassman.[23] [e] Not considered. [f] Log K_- values determined in this study. Values in parentheses are the standard deviation of log $K-$.

Table 3. Summary of Parameters Used for the Determination of Binding Constants for the Sorption of Se on Various Minerals[a]

radionuclide/ solid	A_{sp} (m^2/g)	m/V (g/L)	C_{NR} (M)	I (M)	log K_+[b]	log K_-[b]	log K_1[c]	log K_2[c]	log K_3[c]	log K_4[c]	log K_5[c]	log K_6[c]	log K_7[c]	ref
SeO_4^{2-}/ ferrihydrite	600	0.0264, 0.264	6.7×10^{-7}	0.1 (KCl)	7.29	−8.93	0.65 (0.04)	−	−	−	−	19.46 (0.10)	−	4
SeO_3^{2-}/ ferrihydrite	600	0.0264, 0.264	6.8×10^{-7}	0.1 (KCl)	7.29	−8.93	−	−	−	−	−	26.06 (1.17)	−6.96 (0.64)	4
SeO_3^{2-}/ goethite	49	0.03	2.83×10^{-6}	0.1 (KCl)	7.35	−9.17	−	12.99 (0.07)	18.83 (0.30)	−	−	−	−	3
SeO_4^{2-}/ γ-Al_2O_3	250	1.0	1.42×10^{-4}	0.1 (NaCl)	6.85	−9.05	−	6.70 (0.15)	−	16.72 (1.00)	−	−	−9.32 (0.09)	7
SeO_3^{2-}/ γ-Al_2O_3	250	6.24	2.74×10^{-5}	0.1 (NaCl)	6.85	−9.05	4.74 (0.10)	−	−	−	−	−	−3.70 (0.09)	7
SeO_3^{2-}/ δ-MnO_2	290	0.03, 0.3	6.5×10^{-7}	0.1 (KCl)	−	−3.27	12.20 (0.05)	16.89 (0.66)	−	−	−	−	−	4
SeO_3^{2-}/ anatase	8.6	10	1.25×10^{-4}, 2.5×10^{-5}	0.01 (NaCl)	4.23[d]	−7.49[d]	7.44 (0.04)	11.78 (0.47)	−	−	−	−	−	15
SeO_3^{2-}/ kaolinite[e]	20.5	40	1.9×10^{-5}	0.1 (NaCl)	8.33	−9.73	−	−	16.84 (0.08)	−	−3.80 (0.50)	−	−	8
					−	−7.20	2.37 (0.17)	−	12.54 (0.08)	−	−	−	−	
					8.33	−9.73	2.65 (0.12)	−	16.51 (0.07)	−	−4.35 (0.09)	−	−8.80 (0.05)	
SeO_3^{2-}/ montmorillonite[e]	18.6	40	1.9×10^{-5}	0.1 (NaCl)	−	−7.20	1.50 (0.30)	−	12.20 (0.09)	−	−		−	8

[a] A site density of 2.31 sites/nm^2 (from ref 34) was assigned to all minerals. [b] Acidity constants from Turner and Sassman.[23] [c] Binding constants K_1−K_7 correspond to the following surface reactions: K_1, $\equiv XOH^0 + A^{-z} = \equiv XOH{-}A^{-z}$; K_2, $\equiv XOH^0 + A^{-z} + H^+ = \equiv XOH_2{-}A^{-z+1}$; K_3, $\equiv XOH^0 + A^{-z} + 2H^+ = \equiv XOH_2{-}HA^{-z+2}$; K_4, $\equiv XOH^0 + A^{-z} + 3H^+ = \equiv XOH_2{-}H_2A^{-z+3}$; K_5, $\equiv XOH^0 + A^{-z} = \equiv XO{-}A^{-z-1} + H^+$; K_6, $2(\equiv XOH^0) + A^{-z} + 2H^+ = (\equiv XOH_2)_2{-}A^{-z+2}$; K_7, $2(\equiv XOH^0) + A^{-z} = (\equiv XO)_2{-}A^{-z-2} + 2H^+$, where $A^{-z} = SeO_3^{2-}$ or SeO_4^{2-}. Values in parentheses are standard deviations of the binding constants. [d] Acidity constants for rutile[23] are used. See text. [e] Log K values in the first line for the aluminosilicate minerals are for aluminol−radionuclide surface complexes; those in the second line are for silanol−radionuclide surface complexes.

Table 4. Summary of Parameters Used for the Determination of Binding Constants for the Sorption of TcO_4^- on Minerals[a]

solid	A_{sp} (m^2/g)	m/V (g/L)	C_{NR} (M)	I (M)	log K_+[b]	log K_-[b]	log K_1[c]	log K_2[c]	log K_3[c]	ref
$Mg_6Al_2O_9$[d]	70	0.59	1.4×10^{-5}	0.01	6.85	−9.05	5.97 (0.61)	15.33 (0.23)	−	10
bentonite[e]	10	0.0682	4.2×10^{-14}	0.01	8.33	−9.73	−	−	−1.70 (0.08)	14
					−	−7.20	−	−	−3.50 (0.35)	

[a] A site density of 2.31 sites/nm^2 (from ref 34) was assigned to all minerals. [b] Acidity constants from Turner and Sassman.[23] [c] Binding constants K_1−K_3 correspond to the following surface reactions: K_1, $\equiv XOH^0 + TcO_4^- = \equiv XOH{-}TcO_4^-$; K_2, $\equiv XOH^0 + TcO_4^- + H^+ = \equiv XOH_2{-}TcO_4^0$; K_3, $\equiv XOH^0 + TcO_4^- = \equiv XO{-}TcO_4^{2-} + H^+$. Values in parentheses are standard deviations of the binding constants. [d] Mg/Al layered double hydroxide. [e] Log K values in the first line for bentonite are for aluminol−radionuclide surface species, those in the second line are for silanol−radionuclide surface species.

The strength of the present DLM for predicting the effect of changing system chemistry on anionic radionuclide sorption behavior is demonstrated in Figures 2, 5−7, 9, and 10, where a set of binding constants can accurately represent sorption results under varying geochemical conditions (I, m/V, and C_{RN}).

Effect of pH. The trend of sorption with changing pH for anion adsorption is clearly shown, i.e., anion sorption decreases with increasing pH. This trend is consistent with that of the formation of a protonated surface site, $\equiv XOH_2^+$, at low pH[27] and increasing deprotonation with increasing pH. It is also consistent with the anion sorption behavior analyzed in Dzombak and Morel.[34] This indicates that, in addition to chemical bonding, electrostatic interactions between the anions and the protonated mineral surface play an important role in the adsorption process.

Effects of Aqueous Speciation on Adsorption. The assumption of a single surface complex typically results in a poor model fit to the observed data. Inclusion of multiple surface complexes in the model can usually provide the best fit of the anion sorption data. The complexes formed on the mineral surfaces are expected to be different at different pH values as a

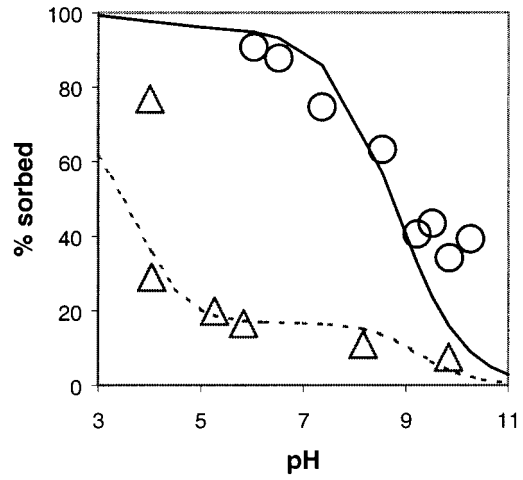

Figure 2. Sorption of I^- on cinnabar. Experimental data are from Balsley et al. (1996)[5] (△, A_{sp} = 1.99 m^2/g, m/V = 1.0 g/L, $[I^-] = 1 \times 10^{-5}$ M, and ionic strength = 0.01 M NaCl) and Ikada et al. (1994)[9] (○, A_{sp} = 1.99 m^2/g, m/V = 10 g/L, $[I^-] = 1 \times 10^{-6}$ M, ionic strength = 0.0003 M). SCM fits to the data of Balsley et al.[5] (dashed line) and Ikada et al.[9] (solid line) are calculated using the parameters listed in Table 2. The surface complexes included in the model are $\equiv HgSH-I^-$ and $\equiv HgSH_2-I^0$.

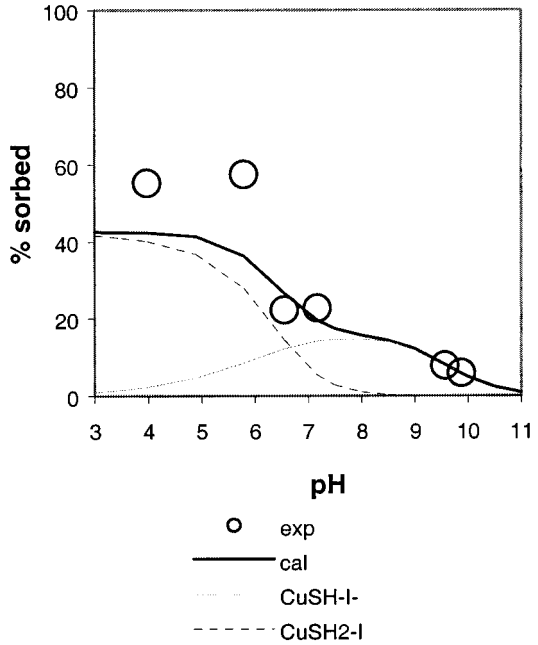

Figure 3. Sorption of I^- on chalcocite. Experimental data are from Balsley et al. (1996)[5] (A_{sp} = 1.11 m^2/g, $[I^-]_{total} = 1 \times 10^{-5}$ M, m/V = 1.0 g/L, I = 0.01 M NaCl), and the solid line is calculated using parameters listed in Table 2. Surface complexes included in the model are $\equiv CuSH-I^-$ and $\equiv CuSH_2-I^0$. Dashed lines represent contributions from the formation of various surface complexes to the total amount of adsorption.

result of changes in aqueous speciation. This effect is most significant for the sorption of SeO_3^{2-}, which has large association constants for the formation of $HSeO_3^-$ (log K_{a1} = 7.3) and H_2SeO_3 (log K_{a2} = 9.9). The results of the speciation analysis in aqueous selenite solution are shown in Figure 15. Protonation of SeO_4^{2-} to form $HSeO_4^-$ (log K_{a1} = 1.9) might also affect the sorption of selenate in acidic solutions (pH < 3). Protonation of pertechnetate, iodide, and iodate is negligible [e.g., log $K_a(HTcO_4) \approx -9$ and log $K_a(HIO_3) = 0.5$], and the primary aqueous species are I^-, IO_3^-, and TcO_4^- in their corresponding solutions.

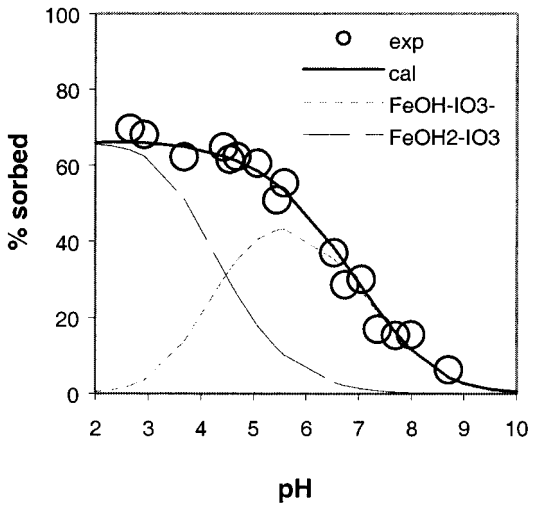

Figure 4. Sorption of IO_3^- on hematite. Experimental data are from Couture and Seitz (1983)[6] (A_{sp} = 10 m^2/g, $[IO_3^-]_{total} = 1.2 \times 10^{-3}$ M, m/V = 58.31 g/L, I = 0.112 M), and the lines are calculated using parameters listed in Table 2. Surface complexes included in the model are $\equiv FeOH-IO_3^-$ and $\equiv FeOH_2-IO_30$. Dashed lines represent contributions from the formation of various surface complexes to the total amount of adsorption.

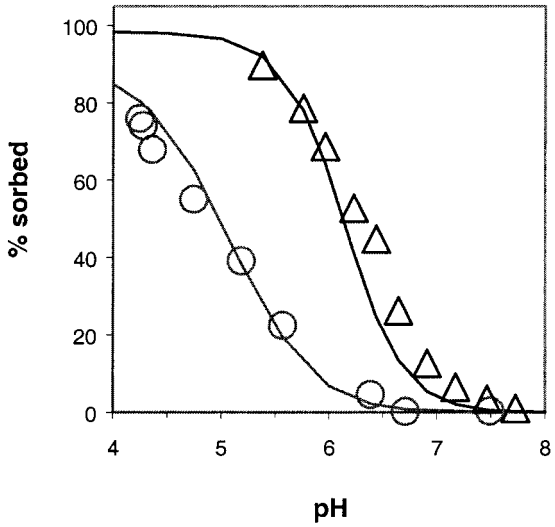

Figure 5. Sorption of selenate on ferrihydrite. The lines are calculated using parameters listed in Tables 1 and 3. Experimental data are from Balistrieri and Chao (1990)[4] (A_{sp} = 600 m^2/g, $[Se(VI)]_{total} = 6.7 \times 10^{-7}$ M, I = 0.1 M KCl): ○, m/V = 0.0264 g/L; △, m/V = 0.264 g/L. Surface complexes included in the model are $\equiv FeO-HSeO_4^{2-}$ and $(\equiv FeOH_2)_2-SeO_4^0$.

Surface complexation reactions that involve different numbers of protons can be included in the model to adjust the pH dependencies of the predicted sorption curves and improve the model results. This is especially the case when stepwise protonation occurs under varying pH conditions, e.g., in the case of selenite. The appropriate selection of surface complexes is crucial to the success of the model in representing sorption results. Including multiple surface complexes (≥3) can improve the quality of the prediction when sorption results are presented over a wide pH range extending to highly acidic (pH ≈ 1) and alkaline (pH ≈ 13) conditions. This is demonstrated for the sorption of selenate on γ-Al_2O_3 (Figure 8) and selenite on kaolinite and montmorillonite (Figures 11 and 12), where three, four, and six surface complexes have been included, respectively. Direct information (EXAFS) is not available on surface com-

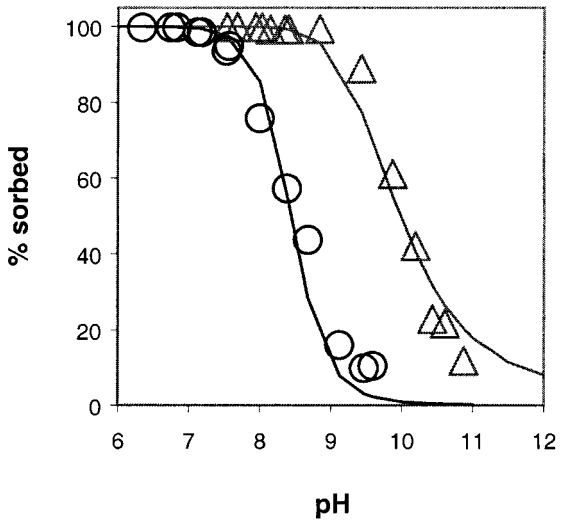

Figure 6. Sorption of selenite on ferrihydrite. The lines are calculated using parameters listed in Tables 1 and 3. Experimental data are from Balistrieri and Chao (1990)[4] (A_{sp} = 600 m^2/g, [Se(IV)]$_{total}$ = 6.8 × 10^{-7} M, I = 0.1 M KCl): ○, m/V = 0.0264 g/L; △, m/V = 0.264 g/L. Surface complexes included in the model are $(\equiv FeOH_2)_2-SeO_30$ and $(\equiv FeO)_2-SeO_3^{4-}$.

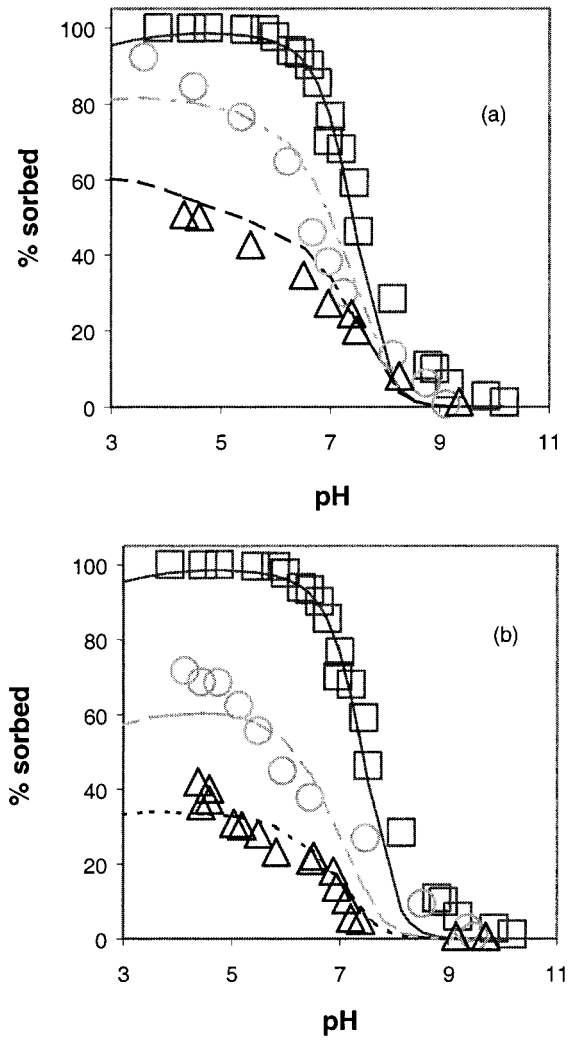

Figure 7. Sorption of selenite on goethite. The lines are calculated using parameters listed in Tables 1 and 3. Surface complexes included in the model are $\equiv FeOH_2-HSeO_3^0$ and $\equiv FeOH-HSeO_3^-$. Experimental data are from Balistrieri and Chao (1987)[3] (A_{sp} = 49 m^2/g, I = 0.1 M KCl). (a) m/V = 0.03 g/L; □, $[SeO_3^{2-}]_{total}$ = 6.5 × 10^{-7} M (solid line); ○, $[SeO_3^{2-}]_{total}$ = 2.83 × 10^{-6} M (dashed−dotted line); △, $[SeO_3^{2-}]_{total}$ = 5.34 × 10^{-6} M (dashed line). (b) $[SeO_3^{2-}]_{total}$ = 6.5 × 10^{-7} M; □, m/V = 0.03 g/L (solid line); ○, m/V = 0.006 g/L (dashed line); △, m/V = 0.003 g/L (dotted line).

plexes for the radionuclide−mineral systems studied here, and the exact form of the surface reaction is postulated to obtain the best fit to the data. A combined analysis of sorption behavior, aqueous speciation, and surface site distribution can assist in the selection of surface complexes. For example, the increase of SeO_3^{2-} sorption with pH in acidic solutions (pH < 5) on kaolinite and montmorillonite (Figures 11 and 12)[8] follows the trend for the formation of $HSeO_3^-$ in this pH range, as shown in the speciation diagram for Se(IV) (Figure 15). Analysis of mineral surface site distribution[27] suggests that aluminosilicate surface sites are protonated in the same pH range to form a positively charged site, $\equiv XOH_2^+$. Thus, surface complexes of the type $\equiv XOH_2-HSeO_3^0$ were included in the model, and the sorption data were well-represented at the low pH range. The contribution to the total amount of adsorption from the formation of each surface complex was localized in a relatively small pH range.

A positive correlation is obtained between the calculated binding constants for the sorption of radionuclide cations and the hydrolysis constants; larger hydrolysis constants result in an increase in the estimated binding constants.[27] A similar trend is also noted in the radionuclide anion sorption. Figure 16 shows an increase in binding constants with increasing first protonation constants of the adsorbing divalent anions, A^{2-} (where A = SeO_4 and SeO_3 in this study). This suggests that anions prone to protonation would also associate with surface sites to form surface complexes. It is not surprising that the logarithms of the binding constants decrease (become less positive or more negative) with increasing negative charge on the postulated surface complexes. Such a trend is also noted by Dzombak and Morel[34] for selenite and selenate and other divalent anions. The binding constants obtained from this study are consistent with the trend obtained by Dzombak and Morel,[34] also using DLM, for the divalent anions, as shown in Figure 16 for surface complexes of the types $\equiv XOH-A^{2-}$ and $\equiv XOH-HA^-$. Because of the limited number of data available for the radionuclide univalent anions (IO_3^-, I^-, and TcO_4^-) and the negligible protonation associated with these anions, it is difficult to perform the correlation for these anions. The development of correlations between adsorption properties and aqueous speciation can significantly improve the predictive capability of the model. These useful correlations will only be possible when extensive sorption data become available for radionuclide anions.

Radionuclide Concentration. The effect of C_{RN} on sorption is shown in Figure 7a for SeO_3^{2-} sorption on goethite and in Figure 9 for the sorption of selenite on γ-Al_2O_3. When the calculated total surface site concentration, T_{XOH}, is of the same order of magnitude as the radionuclide concentration, C_{RN} has a large observable effect on the adsorption. For example, for the adsorption of selenite on goethite (Figure 7a),[3] the T_{XOH} value is 5.64 × 10^{-6} mol of sites/L, as calculated using A_{sp} = 49 m^2/g, m/V = 0.03 g/L, and the assumed value of site density, N_s (2.31 × 10^{18} site/m^2).[23] The C_{RN} values for the three sets of sorption data are 6.5 × 10^{-7} M, 2.83 × 10^{-6} M, and 5.34 × 10^{-6} M. Increased C_{RN} results in reduced adsorption of selenite on goethite. Alternatively,

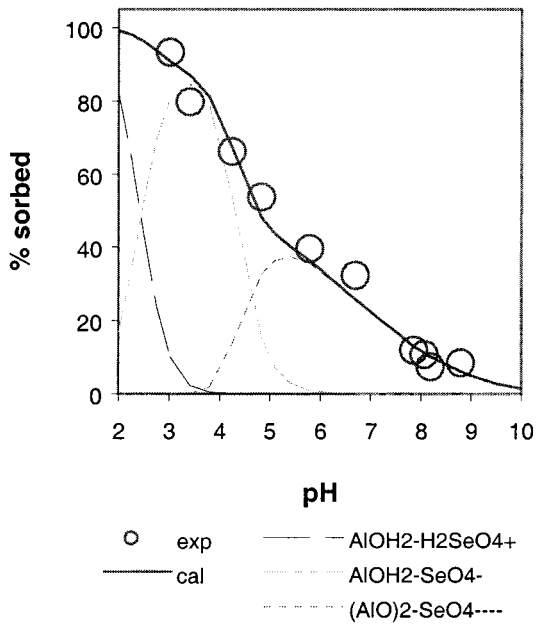

Figure 8. Sorption of selenate on γ-Al_2O_3. The lines are calculated using parameters listed in Tables 1 and 3. Experimental data are from Ghosh et al. (1994)[7] (A_{sp} = 250 m^2/g, m/V = 1.0 g/L, $[SeO_4^{2-}]_{total} = 1.42 \times 10^{-4}$ M, I = 0.1 M NaCl). Surface complexes included in the model are $(\equiv AlO)_2-SeO_4^{4-}$, $\equiv AlOH_2-SeO_4^{-}$, and $\equiv AlOH_2-H_2SeO_4^{+}$. Dashed lines represent contributions from the formation of various surface complexes to the total amount of adsorption.

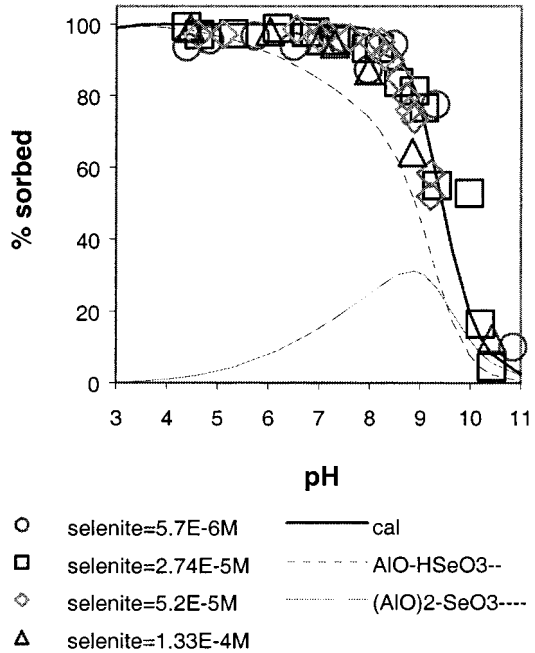

Figure 9. Sorption of selenite on γ-Al_2O_3. The lines are calculated using parameters listed in Tables 1 and 3. Experimental data are from Ghosh et al. (1994)[7] (A_{sp} = 250 m^2/g, m/V = 6.24 g/L, I = 0.1 M NaCl). ○, $[SeO_3^{2-}]_{total} = 5.7 \times 10^{-6}$ M; □, $[SeO_3^{2-}]_{total} = 2.74 \times 10^{-5}$ M; ◇, $[SeO_3^{2-}]_{total} = 5.2 \times 10^{-5}$ M; △, $[SeO_3^{2-}]_{total} = 1.33 \times 10^{-4}$ M. Surface complexes included in the model are $(\equiv AlO)_2-SeO_3^{4-}$ and $\equiv AlO-HseO_3^{2-}$. Dashed lines represent contributions from the formation of various surface complexes to the total amount of adsorption.

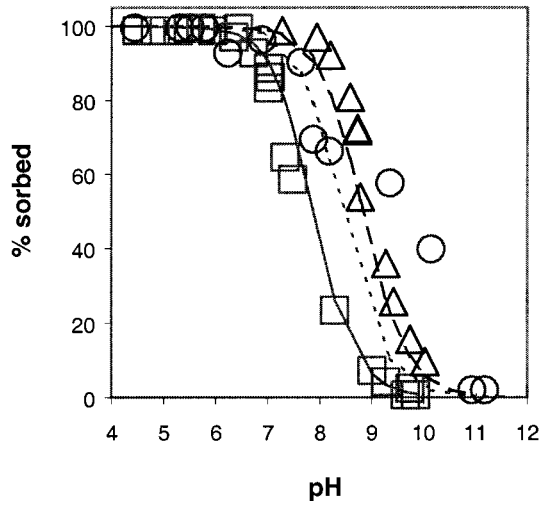

Figure 10. Sorption of selenite on δ-MnO_2. The lines are calculated using parameters listed in Tables 1 and 3. Surface complexes included in the model are $\equiv MnOH_2-SeO_3^{-}$ and $\equiv MnO-HSeO_3^{2-}$. Experimental data are from (i) Balistrieri and Chao (1990)[4] (A_{sp} = 290 m^2/g, $[SeO_3^{2-}]_{total} = 6.5 \times 10^{-7}$ M, I = 0.1 M KCl); □, m/V = 0.03 g/L (solid line); △, m/V = 0.3 g/L (dotted line); and (ii) Saeki et al. (1995)[13] (A_{sp} = 10.2 m^2/g, $[SeO_3^{2-}]_{total} = 1.0 \times 10^{-6}$ M, I = 0.1 M NaCl); ○, m/V = 3.33 g/L (dashed line).

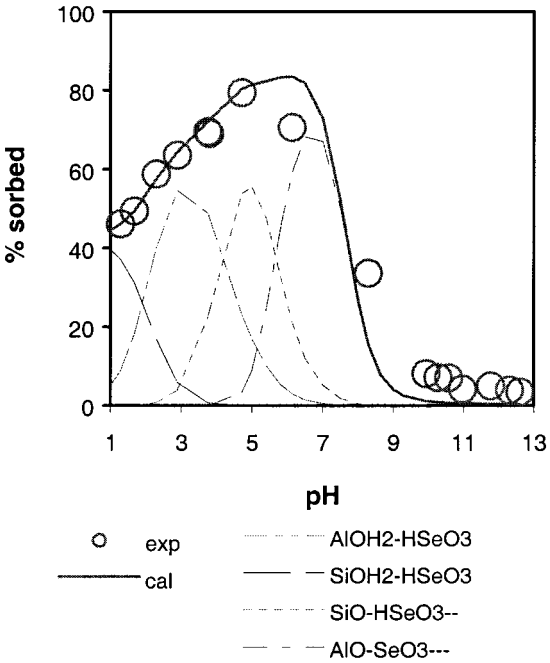

Figure 11. Sorption of selenite on kaolinite. The lines are calculated using parameters listed in Tables 1 and 3. Experimental data are from Goldberg and Glaubig (1988)[8] (A_{sp} = 20.5 m^2/g, m/V = 40 g/L, $[SeO_3^{2-}]_{total} = 1.9 \times 10^{-5}$ M, I = 0.1 M NaCl). Surface complexes included in the model are $\equiv AlOH_2-HSeO_3^{0}$, $\equiv SiOH_2-HSeO_3^{0}$, $\equiv SiO-HSeO_3^{2-}$, and $\equiv AlO-SeO_3^{3-}$. Dashed lines represent contributions from the formation of various surface complexes to the total amount of adsorption.

if the total surface site concentration T_{XOH} is far in excess of C_{RN}, the effect of C_{RN} on sorption is negligible. This is shown in Figure 9 for the sorption of selenite on γ-Al_2O_3,[7] where the T_{XOH} value is 5.98×10^{-3}, whereas the C_{RN} values are from 5.7×10^{-6} to 1.33×10^{-4} M. The sorption curves for the four data sets are identical.

The effects of C_{RN} on sorption behavior can also be predicted using parameters determined in this study. For example, using the parameters in Table 3, the sorption of Se(IV) as SeO_3^{2-} on goethite is calculated as a function of the total selenite concentration at various pH values and is shown in Figure 17. This figure shows a reduction in adsorption with increasing radionuclide concentration, i.e., the same trend that was

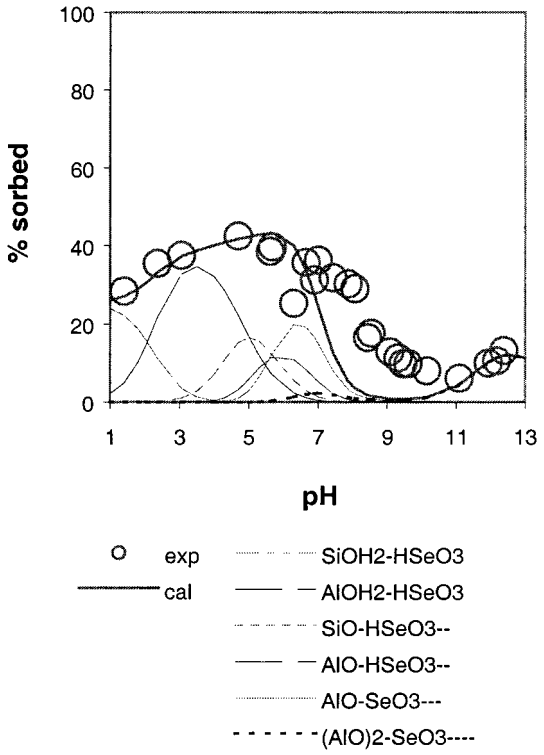

Figure 12. Sorption of selenite on montmorillonite. The lines are calculated using parameters listed in Tables 1 and 3. Experimental data are from Goldberg and Glaubig (1988)[8] (A_{sp} = 18.6 m^2/g, m/V = 40 g/L, $[SeO_3^{2-}]_{total}$ = 1.9 × 10^{-5} M, I = 0.1 M NaCl). Surface complexes included in the model are ≡$AlOH_2$−$HSeO_3^0$, ≡$SiOH_2$−$HSeO_3^0$, ≡AlO−$HSeO_3^{2-}$, ≡SiO−$HSeO_3^{2-}$, ≡AlO−SeO_3^{3-}, and (≡AlO)$_2$−SeO_3^{4-}. Dashed lines represent contributions from the formation of various surface complexes to the total amount of adsorption.

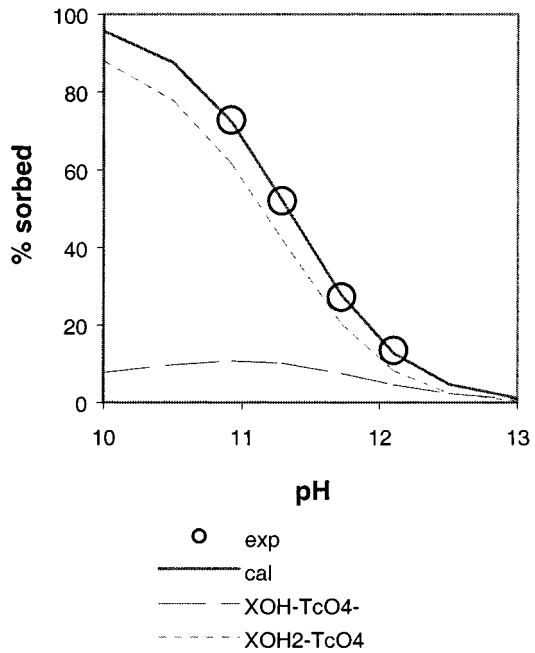

Figure 13. Sorption of pertechnetate on Mg/Al layered double hydroxide ($Mg_2Al_2O_9$). The line is calculated using parameters listed in Table 4. Surface complexes included in the model are ≡$AlOH$−TcO_4^- and ≡$AlOH_2$−TcO_4. Experimental data are from Kang et al. (1996)[10] (A_{sp} = 70 m^2/g, m/V = 0.59 g/L, $[TcO_4^-]_{total}$ = 1.4 × 10^{-5} M, I = 0.01 M). Dashed lines represent contributions from various surface complexes to the total amount of adsorption.

predicted for radionuclide cation adsorption.[27] In contrast to radionuclide cations, for which the adsorption

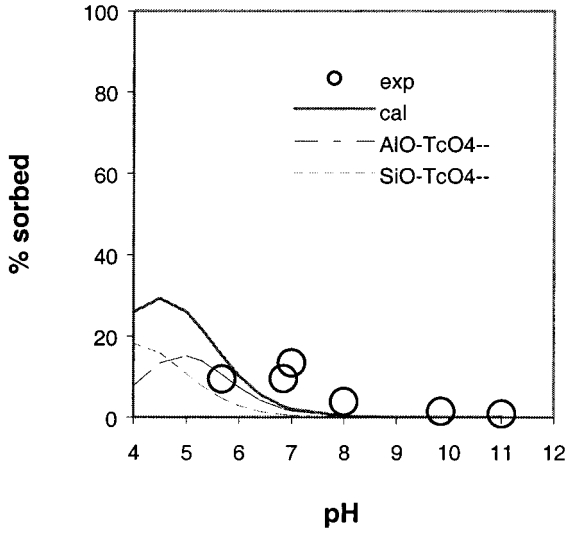

Figure 14. Sorption of pertechnetate on bentonite. The lines are calculated using parameters listed in Table 4. Surface complexes included in the model are ≡AlO−TcO_4^{2-} and ≡SiO−TcO_4^{2-}. Experimental data are from Shade et al. (1984)[14] (A_{sp} = 10 m^2/g, m/V = 0.0682 g/L, $[TcO_4^-]_{total}$ = 4.2 × 10^{-14} M, I = 0.01 M). Dashed lines represent contributions from various surface complexes to the total amount of adsorption.

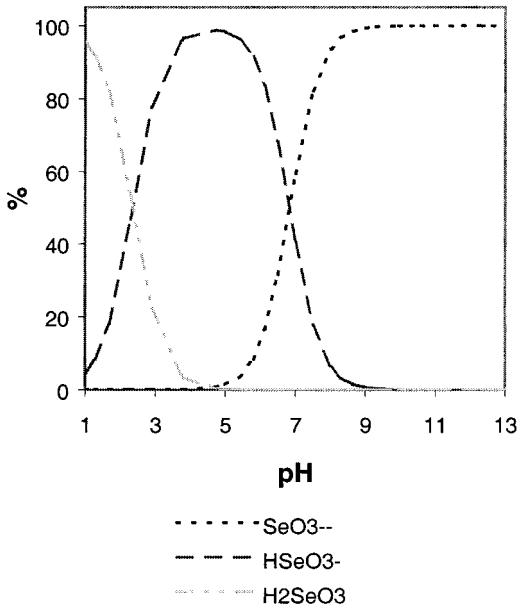

Figure 15. Aqueous-phase speciation diagram for Se(IV). Lines are calculated using thermodynamic data given in Table 1.

is more affected by C_{RN} at higher pH, the effect of C_{RN} on the anion adsorption is more significant at lower pH.

The decreased adsorption with increasing C_{RN} is attributed to a reduction in the number of open sorption sites to levels insufficient for sorbing radionuclides as these sites are filled. When the total concentration of available sorption sites is far in excess of the radionuclide concentration, this effect is negligible. Part of this insensitivity is due to the assumption of a single site type in contrast to the strong site/weak site approach of Dzombak and Morel.[34]

In HLW repository systems, concentrations for cationic radionuclides might be dilute.[28−30] Depending on the number of sorption sites available along the flowpath, C_{RN} might have little effect on the radionuclide adsorption in these systems. Anionic radionuclides, however, have a much higher solubility[28−30] and might

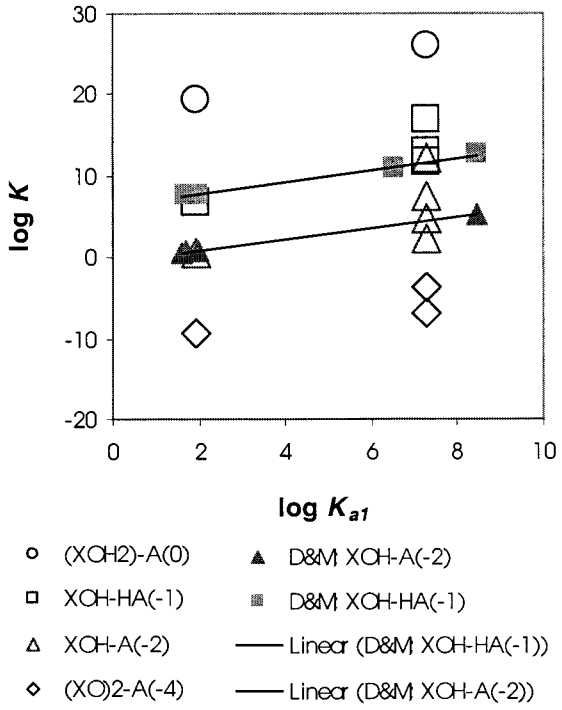

Figure 16. Plot of the binding constants, log K, vs first protonation constants, log K_{a1}, for divalent anions. Open symbols are from this study; solid symbols are taken from Dzombak and Morel.[34]

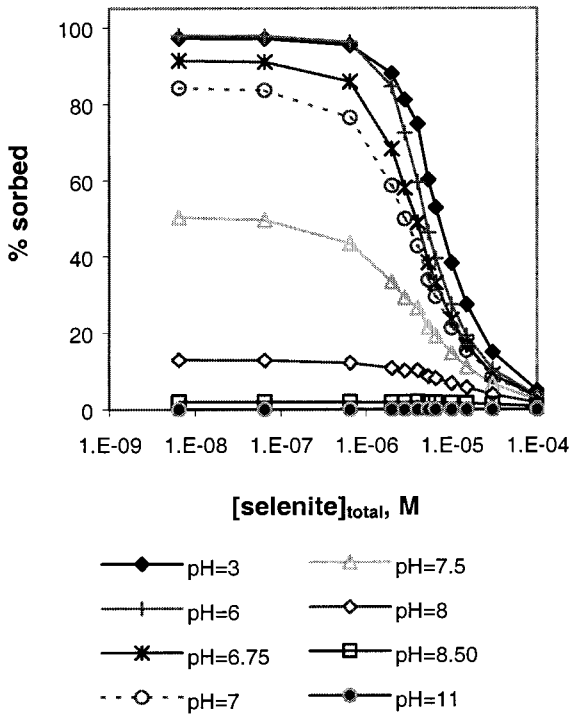

Figure 17. Sorption of Se(IV) on goethite as a function of total selenite concentration at various pH (A_{sp} = 49 m^2/g, m/V = 0.03 g/L, I = 0.1 M KCl). All lines are calculated using parameters in Table 3.

be comparable to T_{XOH}, so that the effects of available sorption sites might be more significant.

Solid Mass-to-Solution Volume Ratio. For a specific mineral, the amount (percent) of adsorbed radionuclide increases as m/V becomes larger. This is demonstrated in Figures 5 and 6 (selenate and selenite, respectively, on ferrihydrite), Figure 7b (selenite on goethite) and in Figure 10 (selenite on δ-MnO_2). This trend is reasonable because the value of m/V is directly

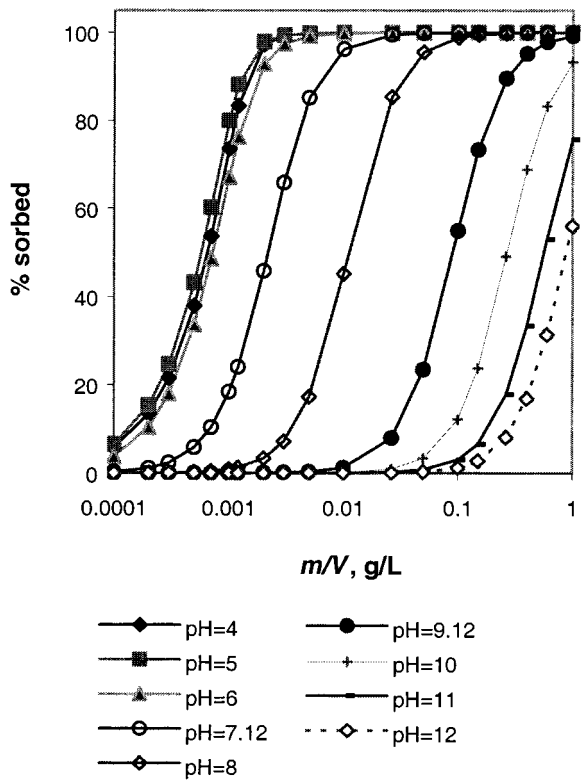

Figure 18. Sorption of selenite on ferrihydrite as a function of m/V at various pH (A_{sp} = 600 m^2/g, $[SeO_3^{2-}]_{total}$ = 6.8 × 10^{-7} M, I = 0.1 M KCl). All lines are calculated using parameters in Table 3.

proportional to the total number of available sorption sites. The greater the number of available sites, the more effective the solid will be in adsorbing the trace concentration of radionuclides.

Using the parameters determined in this study, the present DLM predicts a sorption edge as a function of m/V (Figure 18). As the pH increases, the sorption edge shifts to higher m/V values for the sorption of anionic species. It has been predicted that this sorption edge shifts to lower m/V values for the sorption of cationic species, such as NpO_2^+.[27] Pabalan et al.[24] noted that, when the sorption data are normalized to m/V and presented in terms of a distribution coefficient, K_d, sorption becomes relatively insensitive to the change in solid concentration. This was also seen in our study for modeling the sorption of radionuclide cations.[27] In the present study, the K_d values for the sorption of selenite on goethite are predicted to be insensitive to changes in m/V above neutral pH, but an increase of K_d with m/V becomes obvious at lower pH values, where it appears to approach a stable value, as shown in Figure 19. As m/V increases, the total concentration of available sorption sites, T_{XOH}, increases. When m/V is small and the T_{XOH} values are of the same order of magnitude as the total radionuclide concentration (6.5 × 10^{-7} M for the case shown in Figure 19), the greater m/V (or T_{XOH}) makes the solid more effective in adsorbing the radionuclide, resulting in an increased K_d. As m/V increases and T_{XOH} becomes far in excess of the radionuclide concentration (e.g., T_{XOH} >10^{-5} mol of sites/L), the increased m/V has little influence on the sorption. A similar "threshold" effect was also noted for cation sorption by Pabalan et al.[43] The greater sensitivity of anion adsorption at lower pH to changing m/V is consistent with the results obtained for the effect of C_{RN}

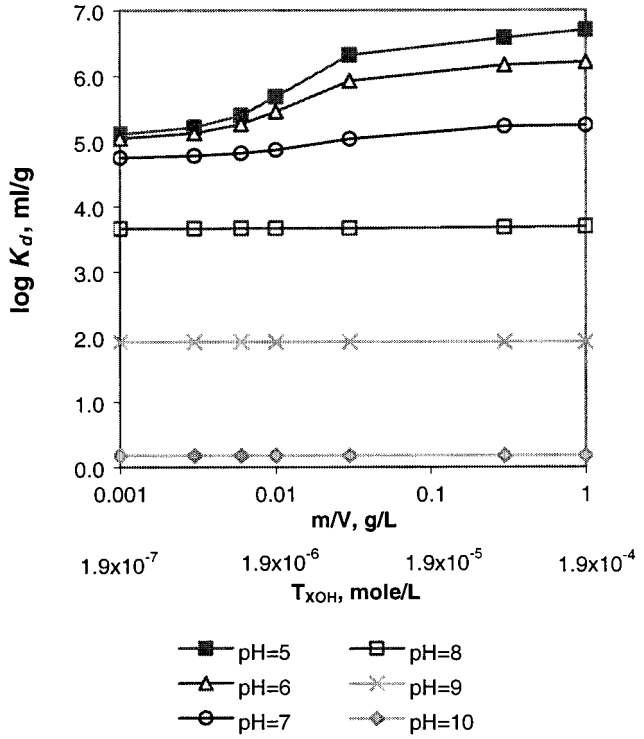

Figure 19. Plot of K_d vs m/V for the sorption of selenite on goethite (A_{sp} = 49 m^2/g, $[SeO_3^{2-}]_{total} = 6.5 \times 10^{-7}$ M, I = 0.1 M KCl). The lines are calculated using parameters in Table 3.

on anion sorption, as described in the previous section. The predicted insensitivity of the cation [e.g., Np(V)] sorption to m/V in our recent study (Figure 18 in ref 25) is due to the extremely small concentration of radionuclide (5.5×10^{-14} M) compared to the total concentration of available sorption sites, which ranges from 10^{-8} to 10^{-4} mol of sites/L and is far beyond the threshold value of m/V. In a radionuclide repository system, even though m/V values are not known with precision, the concept of a threshold value might be useful to constrain sorption in applying SCM approaches to field transport calculations. In the saturated zone, values of m/V are expected to be large in rock-dominated systems, thus yielding T_{XOH} values that are far greater than the trace amount of radionuclides. The m/V might have little effect on K_d values in such systems. In the unsaturated zone, however, wetting might be incomplete, reducing contact with the aquifer minerals (e.g., reducing T_{XOH}). Under these conditions, m/V might be more pronounced.

Valence States. For the radionuclides present in nuclear waste such as Np, Tc, Pu, and U, it has been found[44] that the formation of lower valence states could significantly increase the retardation/adsorption of the nuclide by the host rock. Shown in Figure 20 is the sorption of Se on ferrihydrite.[4] It is seen that the lower valence states [Se(IV)] adsorb more strongly than the higher valence states [Se(VI)].[33] Similar behavior is also observed for the sorption of Se(IV) and Se(VI) on γ-Al_2O_3 (Figures 8 and 9).[7] More importantly, reducing conditions for Tc can result in the changing of speciation from TcO_4^- to TcO^{2+} (anionic to cationic form) which can have a significant enhancing effect on Tc-sorption.[31,32] Moderately reducing conditions have been observed in saturated zone groundwaters near Yucca Mountain,[45,46] but no data are available on Tc(IV) sorption to for allow model calculation.

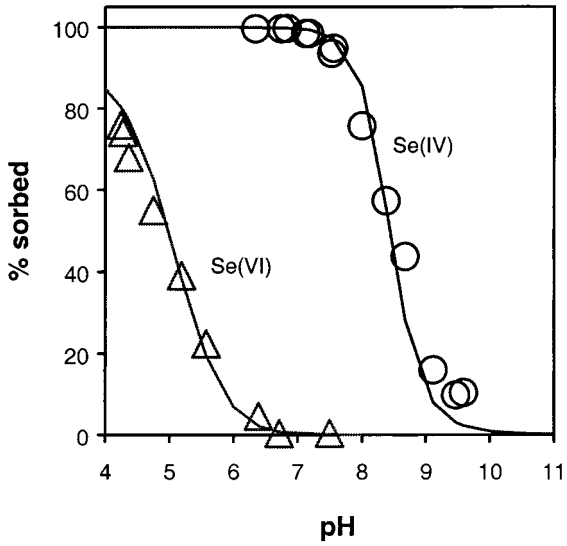

Figure 20. Sorption of Se(IV) and Se(VI) on ferrihydrite. Experimental data are from Balistrieri and Chao (1990)[4] (A_{sp} = 600 m^2/g, m/V = 0.0264 g/L, $[Se]_{total} = 6.7 \times 10^{-7}$ M, I = 0.1 M KCl). The lines are calculated using parameters given in Table 3.

Dependence of Binding Constants on Surface Acidity Constants and Aqueous Thermodynamic Data. As described in a previous paper,[27] the DLM parameters obtained in this work are dependent on the data used in constructing the geochemical equilibrium model for the optimization runs. If acidity constants or aqueous thermodynamic parameters are modified, the radionuclide binding constants must be reevaluated. For example, in the analysis of the results for selenite adsorption on anatase (TiO_2),[15] it was found that the use of DLM intrinsic acidity constants for anatase (log K_+ = 5.37 and log K_- = −5.92), as determined by Turner and Sassman,[23] could not yield a satisfactory fit to the experimental results. Instead, when intrinsic acidity constants for rutile (TiO_2) (logK_+ = 4.23 and logK_- = −7.49) were used in the model, the fit was excellent for data measured at two different selenite concentrations. The pH corresponding to the zero point of charge, pH_{ZPC}, for anatase is 6.1,[47] whereas the relationship

$$pH_{ZPC} = (\log K_+ - \log K_-)/2 \qquad (1)$$

predicts a much lower value of pH_{ZPC} (∼5.6) based on Turner and Sassman's[23] values for anatase. Sprycha[47] obtained log K_+ and log K_- values in the vicinity of 3.1 and −8.9, respectively, and Gruebel et al.[15] determined these values to be 3.6 and −7.6, respectively. It is clear that the intrinsic acidity constants for anatase are largely uncertain, and it is reasonable to use an average of values reported by different authors before the uncertainty is resolved. The results of the modeling for the sorption of SeO_3^{2-} on anatase are shown in Figure 21. The radionuclide binding constants determined from this study will be recalculated when the existing acidity constants are modified by incorporating new potentiometric titration data. Likewise, any significant changes in the aqueous thermodynamic data will require a recalculation of the necessary parameters.

4. Implication of The Modeling Results

Anionic radionuclides are potentially important contributors to dosind in HLW. Anion sorption might reduce radionuclide concentrations and delay arrival

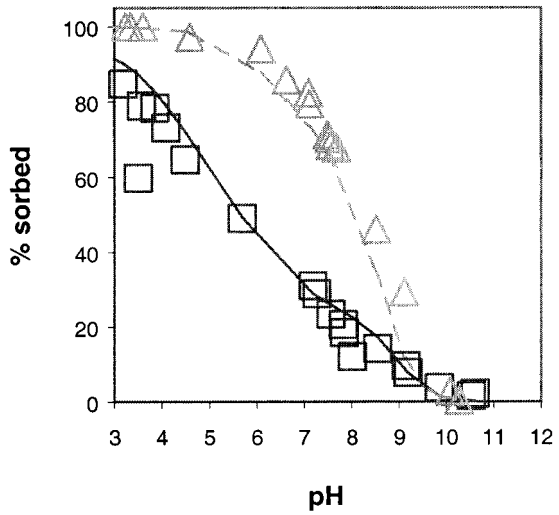

Figure 21. Sorption of selenite on anatase (TiO_2). The lines are calculated using parameters listed in Tables 1 and 3. Experimental data are from Gruebel et al. (1995)[15] (A_{sp} = 8.6 m^2/g, m/V = 10 g/L, I = 0.01 M NaCl): □, $[SeO_3^{2-}]_{total} = 1.25 \times 10^{-4}$ M (solid line); △, $[SeO_3^{2-}]_{total} = 2.5 \times 10^{-5}$ M (dashed line). Surface complexes included in the model are $\equiv TiO-HSeO_3^{2-}$ and $\equiv TiOH-HSeO_3^{-}$.

times at the point of exposure. Because anion sorption behavior is strongly dependent on geochemical conditions along groundwater flow paths, detailed process-level models can provide a level of understanding that is necessary to support transport simulations.

The success of the DLM in predicting the experimental sorption results suggests that it might be possible to use the simple conceptual models developed in this study to extrapolate to a variety of chemical conditions from a relatively limited data set. This is in contrast to typical empirical approaches, where the lack of a strong theoretical basis frequently makes extrapolation beyond experimental conditions uncertain. The results obtained in this work can be used to support parameter values in high-level waste abatement modeling under site-specific hydrochemical conditions.[48] Where detailed information is not available, it might also be possible to use the modeling approach outlined here to provide bounding constraints on radionuclide anion sorption. Although this is not an explicit incorporation of geochemistry in the transport calculations, it does provide a step toward a much sounder theoretical basis for sorption modeling in HLW analyses.

Acknowledgment

This manuscript was prepared to document work performed for the Center for Nuclear Waste Regulatory Analyses (CNWRA) and the U.S. Nuclear Regulatory Commission (NRC). The manuscript is an independent product of the authors and does not necessarily reflect the views or regulatory position of the NRC. CNWRA-generated original data contained here meet quality assurance requirements described in the CNWRA Quality Assurance Manual. The assistance provided by Dr. Roberto T. Pabalan of CNWRA is greatly appreciated.

Literature Cited

(1) *Total System Performance Assessment—Viability Assessment (TSPA-VA) Analyses Technical Basis Document*; Report B00000000-01717-4301 REV 01; Civilian Radioactive Waste Management System Management and Operating Contractor: Las Vegas, NV, 1998.

(2) *Total System Performance Assessment for the Site Recommendation*; Report TDF-WIS-PA-00001 REV 00; Civilian Radioactive Waste Management System Management and Operating Contractor: Las Vegas, NV, 2000.

(3) Balistrieri, L. S.; Chao, T. T. Selenium Adsorption by Goethite. *Soil Sci. Soc. Am. J.* **1987**, *51*, 1145.

(4) Balistrieri, L. S.; Chao, T. T. Adsorption of Selenium by Amorphous Iron Oxyhydroxide and Manganese Dioxide. *Geochim. Cosmochim. Acta* **1990**, *54*, 739.

(5) Balsley, S. D.; Brady, P. V.; Krumhansl, J. L.; Anderson, H. L. Iodide Retention by Metal Sulfides: Cinnabar and Chalcocite. *Environ. Sci. Technol.* **1996**, *30*, 3025.

(6) Couture, R. A.; Seitz, M.G. Sorption of Anions of Iodine by Iron Oxides and Kaolinite. *Nucl. Chem. Waste Manage.* **1983**, *4*, 301.

(7) Ghosh, M. M.; Cox, C. D.; Yuan-Pan, J. R. Adsorption of Selenium on Hydrous Alumina. *Environ. Prog.* **1994**, *13*, 79.

(8) Goldberg, S.; Glaubig, R. A. Anion Sorption on a Calcareous, Montmorillonitic Soil—Selenium. *Soil Sci. Soc. Am. J.* **1988**, *52*, 954.

(9) Ikeda, Y.; Sazarashi, M.; Tsuji, M.; Seki, R.; Yoshikawa, H. Adsorption of I^- Ions on Cinnabar for ^{129}I Waste Management. *Radiochim. Acta* **1994**, *65*, 195.

(10) Kang, M. J.; Rhee, S. W.; Moon, H.; Neck, V.; Fanghanel, Th. Sorption of MO_4^- (M = Tc, Re) on Mg/Al Layered Double Hydroxide by Anion Exchange. *Radiochim. Acta* **1996**, *75*, 169.

(11) Palmer, D. A.; Meyer, R. E. Adsorption of Technetium on Selected Inorganic Ion-Exchange Materials and on a Range of Naturally Occurring Minerals Using Oxic Conditions. *J. Inorg. Nucl. Chem.* **1981**, *43*, 2979.

(12) Parida, K. M.; Gorai, B.; Das, N. N.; Rao, S. B. Studies on Ferric Oxide Hydroxides. III. Adsorption of Selenite on Different Forms of Iron Oxyhydroxides. *J. Colloid Interface Sci.* **1997**, *185*, 355.

(13) Saeki, K.; Matsumoto, S.; Tatsukawa, R. Selenite Adsorption by Manganese Oxides. *Soil Sci.* **1990**, *160*, 265.

(14) Shade, J. W.; Ames, L. L.; McGrarrah, J. E. Actinide and technetium sorption on iron silicate and dispersed clay colloids. In *ACS Symposium Series* 246; American Chemical Society: Washington, D.C., 1984; pp 67—77.

(15) Gruebel, K. A.; Davis, J. A.; Leckie, J. O. Kinetics of Oxidation of Selenite to Selenate in the Presence of Oxygen, Titania, and Light. *Environ. Sci. Technol.* **1995**, *29*, 586.

(16) Zhang, P.; Sparks, D. L. Kinetics of Selenate and Selenite Adsorption/Desorption at the Goethite/Water Interface. *Environ. Sci. Technol.* **1990**, *24*, 1848.

(17) Kent, D. B.; Tripathi, V. S.; Ball, N. B.; Leckie, J. O. *Surface-complexation Modeling of Radionuclide Adsorption in Subsurface Environments*; Technical Report No. 294; Department of Civil Engineering, Stanford University: Stanford, CA, , 1986.

(18) Payne, T. E.; Waite, T. D. Surface Complexation Modeling of Uranium Sorption Data Obtained by Isotope Exchange Techniques. *Radiochim. Acta* **1991**, *52/53*, 487.

(19) Venkataramani, B.; Gupta, A. R. Effect of Anions on the Sorption of Uranyl Ions on Hydrous Oxides: Application of the Surface Hydrolysis Model. *Colloids Surf.* **1991**, *53*, 1.

(20) Bradbury, M. H.; Baeyens, B. A General Application of Surface Complexation to Modeling Radionuclide Sorption in Natural Systems. *J. Colloid Interface Sci.* **1993**, *158*, 364.

(21) Turner, D. R. *A Uniform Approach to Surface Complexation Modeling of Radionuclide Sorption*; Report 95-001; Center for Nuclear Waste Regulatory Analyses: San Antonio, TX, 1995.

(22) Turner, G. D.; Zachara, J. M.; McKinley, J. P.; Smith, S. C. Surface-charge Properties and UO_2^{+2} Adsorption of a Surface Smectite. *Geochim. Cosmochim. Acta* **1996**, *60*, 3399.

(23) Turner, D. R.; Sassman, S. A. Approaches to Sorption Modeling for High-Level Waste Performance Assessment. *J. Contam. Hydrol.* **1996**, *21*, 311.

(24) Pabalan, R. T.; Turner, D. R.; Bertetti, F. P.; Prikryl, J. D. Uranium^{VI} sorption onto selected mineral surfaces: Key geochemical parameters. In *Adsorption of Metals by Geomedia*; Jenne, E. A., Ed.; Academic Press: New York, 1998; pp 99—130.

(25) Turner, D. R.; Pablan, R. T.; Bertetti, F. P. Neptunium(V) Sorption on Montmorillonite: An Experimental and Surface Complexation Modeling Study. *Clays Clay Miner.* **1998**, *46*, 256—269

(26) Helgeson, H. C. Thermodynamics of Hydrothermal Systems at Elevated Temperatures and Pressures. *Am. J. Sci.* **1969**, *267*, 729.

(27) Wang, P.; Anderko, A.; Turner, D. R. Thermodynamic modeling of adsorption of radionuclide on selected minerals: I. Cations. *Ind. Eng. Chem. Res.* **2001**, *40*, 4428.

(28) U.S. Department of Energy. *Viability Assessment of a Repository at Yucca Mountain, Nevada*; Report No. DOE/RW-0508; Office of Civilian Radioactive Waste Management, U.S. Department of Energy: Washington, D.C., 1998.

(29) Nuclear Regulatory Commission. *NRC Sensitivity and Uncertainty Analyses for a Proposed HLW Repository at Yucca Mountain, Nevada, Using TPA 3.1. Conceptual Models and Data*; Report No. NUREG-1668; U.S. Nuclear Regulatory Commission: Rockville, MD, 1999, Vol. 1.

(30) Nuclear Regulatory Commission. *NRC Sensitivity and Uncertainty Analyses for a Proposed HLW Repository at Yucca Mountain, Nevada, Using TPA 3.1. Results and Conclusions*; Report No. NUREG-1668; U.S. Nuclear Regulatory Commission: Rockville, MD, 1999, Vol. 2.

(31) Lieser, K. H.; Bauscher, C. H. Technetium in the hydrosphere and in the geosphere. II. Influence of pH, of complexing agents and of some minerals on the sorption of technetium. *Radiochimica Acta* **1988**, *44*/*45*, 125.

(32) Pabalan, R. T.; Turner, D. R.; Miklas, M. P., Jr. Technetium-99 chemistry in reduced groundwaters: Implications for the performance of a proposed high-level nuclear waste repository at Yucca Mountain, Nevada. In *Materials Research Society Symposium Proceedings: Scientific Basis for Nuclear Waste Management*−*XXIII*; Shoesmith, D., Smith, R., Eds.; Materials Research Society: Warrendale, PA, 2000, Vol. 608, pp 231−236.

(33) Davis, J. A.; Kent, D. B.; Rea, B. A.; Maest, A. S.; Garabedian, S. P. Influence of redox environment and aqueous speciation on metal transport in groundwater: Preliminary results of trace injection studies. In *Metals in Groundwater*; Allen, H. E., Perdue, E. M., Brown, D. S.; Lewis Publishers: Boca Raton, FL, 1993; pp 223−273.

(34) Dzombak, D. A.; Morel, F. M. M. *Surface Complexation Modeling: Hydrous Ferric Oxide*; John Wiley & Sons: New York, 1990.

(35) Davis, J. A.; Kent, D. B. Surface complexation modeling in aqueous geochemistry. In *Mineral*−*water Interface Geochemistry*; Hochella, M. F., Jr., White, A. F., Eds.; Reviews in Mineralogy 23; Mineralogical Society of America: Washington, D.C., 1990; pp 177−260.

(36) Westall, J. C. *FITEQL: A Computer Program for Determination of Chemical Equilibrium Constants from Experimental Data*, version 1.2; Report 82-01; Department of Chemistry, Oregon State University; Corvallis, OR, 1982.

(37) Westall, J. C. *FITEQL: A Computer Program for Determination of Chemical Equilibrium Constants from Experimental Data*, version 2.0; Report 82-02; Department of Chemistry, Oregon State University; Corvallis, OR, 1982.

(38) Wolery, T. J. *EQ3/6, A Software Package for Geochemical Modeling of Aqueous Systems: Package Overview and Installation Guide*, version 7.0; Lawrence Livermore National Laboratory: Livermore, CA, 1992.

(39) Wolery, T. J. *EQ3NR, A Computer Program for Geochemical Modeling of Aqueous-Speciation-Solubility Calculations: Theoretical Manual, User's Guide, and Related Documentation*, version 7.0; Lawrence Livermore National Laboratory: Livermore, CA, 1992.

(40) Hakem, N.; Fourest, B.; Guillaumont, R.; Marmier, N. Sorption of Iodine and Cesium on Some Mineral Oxide Colloids. *Radiochim. Acta* **1996**, *74*, 225.

(41) Anderko, A.; Shuler, P. A computational approach to predicting the formation of iron sulfide species using stability diagrams. *Comput. Geosci.* **1997**, *23*, 647.

(42) Baes, C. F.; Mesmer, R. E. *The Hydrolysis of Cations*; John Wiley & Sons: New York, 1976.

(43) Pabalan, R. T.; Turner, D. R. Sorption modeling for HLW performance assessment. In *NRC High-Level Radioactive Waste Research at CNWRA*; Sagar, B., Ed.; Report No. CNWRA 93-02S; Center for Nuclear Waste Regulatory Analyses: San Antonio, TX, 1993; pp 6-1 to 6-23.

(44) Meyer, R. E.; Arnold, W. D.; Case, F. I.*Valence Effects on the Sorption of Nuclides on Rocks and Minerals. II*; Report No. NUREG/CR-4114, ORNL-6137; Oak Ridge National Laboratory: Oak Ridge, TN, 1985.

(45) Ogard, A. E.; Kerrisk, J. F. *Groundwater Chemistry Along Flow Paths Between A Proposed Repository Site and the Accessible Environment*; Report LA-10188-MS; Los Alamos National Laboratory: Nos Alamos, NM, 1984.

(46) U.S. Department of Energy. *Downhole Eh and pH Measurements for UE*−*25 WT#17*, 1999. Available at http://m-oext.ymp.gov/cgi-bin/prod/db_tdp/atdt/get_tdif.exe?dtn_num=LAAM831311AQ98.003.

(47) Sprycha, R. Surface Charge and Adsorption of Background Electrolyte Ions at Anatase/Electrolyte Interface. *J. Colloid Interface Sci.* **1984**, *102*, 173.

(48) Turner, D. R.; Pabalan, R. T. Abstraction of mechanistic sorption model results for performance assessment calculations at Yucca Mountain, Nevada. *Waste Manage.* **1999**, *19*, 375.

Received for review November 21, 2000
Revised manuscript received July 12, 2001
Accepted July 19, 2001

IE000992H